

Antiquark nuggets as dark matter: Detection prospects with the ANITA telescope

B. Rotter* for the ANITA collaboration

University of Hawaii at Manoa

E-mail: brotter@phys.hawaii.edu

Regions of parameter space for a nearly forty year old hypothesis explaining dark matter with the existence of heavy composite quark objects remain unexplored. The Antarctic Impulsive Transient Antenna (ANITA) telescope, a NASA-sponsored long duration balloon payload, is in a unique position to test this exotic dark matter candidate by exploiting the sensitivity of an on-board monitoring subsystem. We present estimates of the experimental sensitivity of ANITA to these dark matter candidates, and estimates for the three flights of the payload to date.

*The 34th International Cosmic Ray Conference,
30 July- 6 August, 2015
The Hague, The Netherlands*

*Speaker.

1. Introduction

The existence of a halo of non-luminous weakly interacting matter encompassing galaxies has strong experimental evidence, with total quantities surpassing the cumulative total of all currently observed matter in the universe.[1] The composition of this matter remains an unanswered question in the particle astrophysics community. Many current theories favor non-baryonic particles beyond the standard model, however several candidate particles which have not been experimentally excluded across all parameter space still exist within the current standard model regime.

To remain a viable candidate, any standard model particle must have a low enough flux to have remained undetected by current generation particle detectors. This requires it to be much more massive than the often probed \lesssim TeV dark matter energy scale. Particles in this lower mass region of $B \sim 10^3 - 10^{25}$ have already been constrained, yet higher masses, whose low flux requires alternate indirect detection techniques, remain to be probed. Current limits on this non-luminous matter set the interaction cross section per unit mass to $\sigma/M \lesssim 0.1 \text{cm}^2 \text{g}^{-1}$. [5] [6] This limit is satisfiable by nuclear density objects with macroscopic masses.

2. Antiquark Nuggets (AQNs)

Quark nuggets (QNs) were first theorized in the mid 80's as a compact strangelet object[4]. These very massive, high baryon number objects would fit into the parameter space left vacant by modern and historical observations. Additional recent work has theorized a survival mechanism for these particles through the nucleosynthesis period in early universe formation, initially thought to be a strong constraint, which would allow them to persist to the current day.[3] A new application of the model also includes the additional generation of an anti-quark nugget (AQN) at a ratio of 3 AQN : 2 QN, which is allowable due to their formation in the early universe before the origin of the matter-antimatter asymmetry.[7, 8, 9, 10] These anti-matter particles, isotropically distributed as some fraction of the total dark matter flux, will annihilate with large massive bodies, such as the earth, and emit an indirect signal with which their flux can be measured.

Due to their non-relativistic velocities, compact standard matter QN objects would leave only a seismic disturbance, as well as a slight thermal energy transfer, in their interaction path as they collide with matter already existing in the interaction medium. Seismic measurements from the Apollo 11 mission set a limit on these QN particle interactions. Additional limits on the flux are set by thermal deposition inside the Earth and Sun, an unobserved low energy neutrino flux from annihilating AQN particles, and measurements of fast-meteors, which are summarized in Figure 1.

3. Detectable AQN signatures

AQNs moving through a medium would have an annihilation driven radiative emission signature. This annihilation of an AQN will emit un-polarized photons isotropically in a track moving through the medium with the velocity of the particle. This radiative component is the avenue in which the ANITA telescope will be able to observe such an object, visible as an increase in thermal RF noise power in the direction of the particle moving with some angular velocity across the field of view of the detector. A mean 240km/s Maxwell velocity distribution of the virialized dark

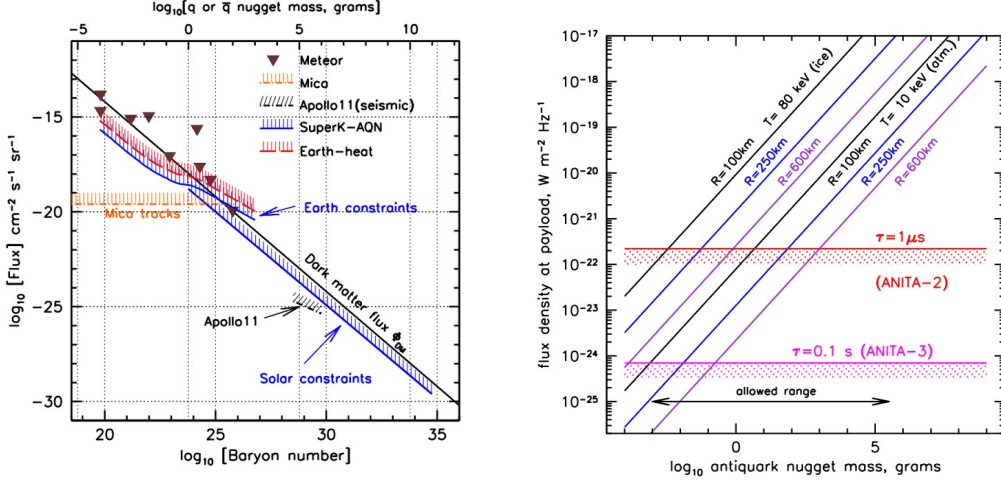


Figure 1: (left) Constraints on AQN Flux via various historical and contemporary measurements, including expected Dark Matter density, low energy neutrino flux, and lunar seismic measurements[14] (right) Energy Flux Density of AQN particles of varying annihilation surface temperatures (T) and distances from payload (R) as a function of mass. Includes estimated minimum detectable signal power of ANITA2 and ANITA3 instruments [2]

matter halo would give the objects a unique characteristic velocity not shared by anthropogenic sources, such as aircraft and satellites, nor celestial objects, such as meteors entering and thermally radiating within the atmosphere.

The radio flux density emitted by such a particle (equation 3.1) has a largely flat spectral density in the bandwidth of interest[2]. It is governed by the effective surface temperature (T) of such an object accreting normal matter, the distance D from the detector, and the mass (directly related to baryon number B). [10]

$$S_{AQN,atm} \sim 8 \times 10^{-23} W m^{-2} H^{-1} \left(\frac{T}{10 \text{ keV}} \right)^{13/4} \left(\frac{\langle D \rangle}{100 \text{ km}} \right)^{-2} \left(\frac{B}{10^{24}} \right)^{2/3} \quad (3.1)$$

Further discussion of limits on maximum surface temperature of an AQN, set by a requirement that the radiation pressure just outside the surface of the AQN can not exceed a level required to accelerate accreting matter away from the path, can be found in [2]. This temperature varies by the density of the accretion medium through which the AQN is transiting. AQN particles annihilating in the ice sheet of the Antarctic continent would have a larger radiated power, scaled by the Fresnel coefficient of leaving the ice-air interface and the attenuation length of radio in ice, and would thus also be detectable. However, the much larger volumetric area afforded by the atmosphere allows a larger observable AQN interaction quantity.

The broadband radio signature of an AQN particle annihilating in the atmosphere is strong in comparison to the $P \lesssim 5 \text{ pW}$ thermal noise power from the ANITA electronics system temperature. Factoring in the antenna gain and bandwidth of the ANITA instrument, a wide range of AQN masses and distances will be visible from the payload(see Fig 1). Signal on this scale is there-



Figure 2: The ANITA2 (left) and ANITA3 (right) instruments before launch. ANITA 2 is seen hanging from launch vehicle at the Long Duration Balloon Facility outside McMurdo Station Antarctica, 2008. The eight nadir ring antennas, stowed for launch, are deployed in this photo (Photo courtesy of Ryan Nichol) The ANITA3 instrument is seen sitting on a testing "dance floor", also outside McMurdo Station, Antarctica, in 2015. Note that the nadir ring of 16 antennas is obscured by the stowed solar panel ring.(Photo by author)

fore detectable by the electronics aboard the ANITA telescope, making a search for this candidate particle an interesting prospect.

If one assumes an equal distribution dark matter fraction per nucleon mass as an AQN mass distribution, one can derive expected rates of particles incident at earth from the assumed local average dark matter density of 0.3 GeV cm^{-3} and an isotropic flux through the $\sim 720 \text{ km}^2$ target area visible from a sub-orbital observation platform such as ANITA. At $B \sim 10^{24}$, the rate is high, at ~ 10 interactions/second in the field of view. This rate falls exponentially, and reaches only one expected event per an example 25 day flight at $B \sim 10^{32}$, which will set the absolute upper limit for detectability.

4. ANITA telescope platform

Beginning with the first full mission in 2006, there have been three full scale ANITA balloon flights yielding a cumulative 85 days of total observation time.[12] Upgrades to sensitivity were made for each flight, further improving upon the main science mission of measuring the UHE neutrino flux while also sequentially increasing the total observation time for the platform. This work focuses on the ANITA2 and ANITA3 telescopes due to their identical power monitor systems, the latter of which was improved with this AQN search specifically in mind.

The ANITA instrument comprises an array of dual polarized broad band radio frequency (RF) horn antennas oriented pointing radially outwards, creating a full 360° azimuthal field of view. These antennas are arranged into sets to create 16 "phi sectors", each with a half power beamwidth of 30° . The antennas within a phi sector are stacked vertically with a goal of maintaining the

same azimuth and elevation coverage.(Figure 2) The elevation and azimuthal opening angles of the antennas are comparable, yielding an observation solid angle of $\Omega \sim 3\text{sr}$.

The ANITA2 flight instrument had 40 total antennas, with two or three (alternating) antennas per phi sector. This was an improvement over the ANITA1 flight, which had only 32 antennas (two per phi sector). This was increased once more for the ANITA3 flight(Figure 2), which added an additional 8 antennas to the nadir ring, giving every phi sector three antennas. The additional antennas were made possible by devising a robust "drop down" system that allowed the payload to expand past the allowable size restrictions immediately after launch. Each additional antenna allows, in this analysis, for the directional power averaging to be increased, lowering the minimum radio flux sensitivity bound.

The electric field incident on these antennas are heavily amplified and band passed, with a 1GHz bandwidth from $\sim 200\text{MHz}$ to 1.2GHz , through in-line analog filters in order to observe faint RF signals without adding significant additional system noise. These independent signal chains are then run through co-axial cables to the instrument box, where they are digitized by both a high speed 2.6Gs/s analog to digital converter, the LABRADOR 3 ASIC, and a "long" integration time log-power detector (Figure 3). This data is stored along side GPS heading, location and tilt information, as well as numerous other diagnostic and temperature readouts, in one of three 6TB storage vaults on the payload.

The instrument is launched from McMurdo Station, Antarctica to an altitude of $\sim 120\text{kft}$ using a NASA Long Duration Balloon. The circumpolar vortex present over continent allows for a long observation duration (on the order of one month) without the flight path deviating outwards over the ocean, where recovery would become impossible. This gives the detector a field of view of nearly one million km^2 of the ice sheet at any time, as well as any view of particles impacting the atmosphere. The ice acts as a transparent, dense interaction medium, in which particle interactions have a much higher cross section while the emitted radiation maintains its long attenuation length.

The high speed waveform digitizer, the primary science detector system, has an extremely low duty cycle measurement (100ns readout windows taken at an unbiased 1Hz) which prevents it from being used in a AQN search as a precise detector of RF power. The noise (σ_{noise}) is inversely related to the integration time by $1/\sqrt{\tau}$, and as such the relatively low signal AQN emission tracks strongly favor a much longer integration window for detection.

There remains an additional digitized signal path, the power monitor subsystem, which was initially designed to be used as a monitor for the health and consistency of the signal chain. It has proven sensitive to small fluctuations of RF power primarily due to its long integration time. In addition to visualizing consistent sources of RF power present in the field of view of the detector, it is able to attempt this preliminary search for AQNs.

5. Power monitor subsystem

In both flights, signal is coupled off from the main digitizer path and fed into a dedicated power detection circuit(Figure 3). For the ANITA2 and ANITA3 flights, the broad band signal from this path was converted to a power level then integrated via a low pass RC filter before being digitized. This was done via a MAX4003 broad band RF detector chip whose output was sampled by a LTC1415 12-bit 1.25Msps analog to digital converter. Due to power, cost, and space constraints,

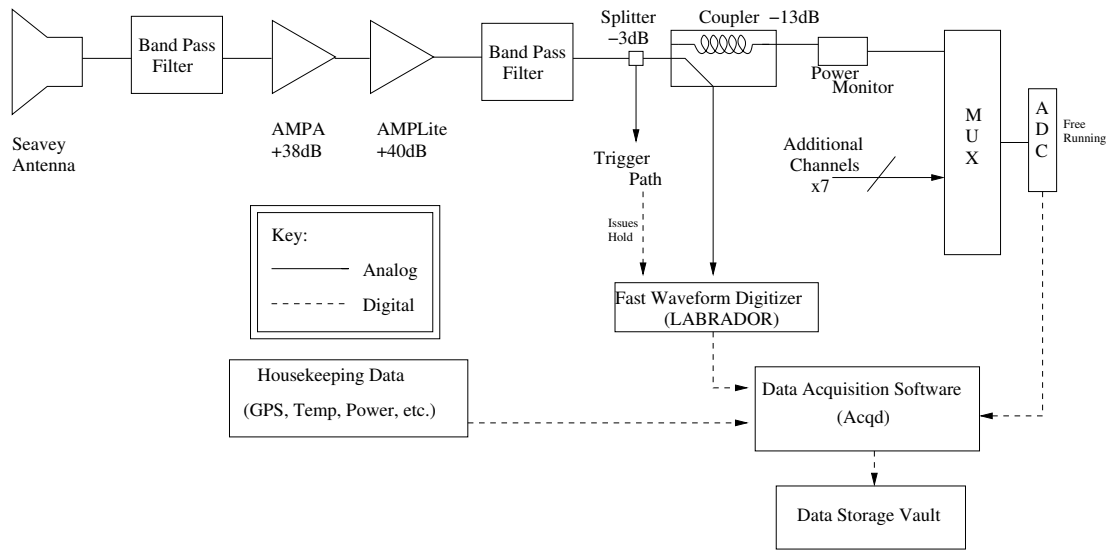


Figure 3: Signal chain for an individual channel path in the ANITA2 and ANITA3 telescopes

the output log power was fed into a switch multiplexer with seven other channels, which results in an equal occupancy round robin sampling of the power for all channels. The MAX4003 outputs a DC voltage proportional to the logarithm of the RF power (dBm), which is then measured by the ADC.

The ANITA2 electronics did not take advantage of the fast sampling rate of the LTC1415, and as thus only can utilize the relatively short analog integration time of $1\mu\text{s}$ digitized at 10Hz. The ANITA3 readout firmware corrected this oversight by digitally averaging 5265 samples of each channel before reading out the value, increasing integration time to 5ms, which was then digitized at 20Hz. This improvement tightens the theoretical sensitivity while only increasing the already fractionally small data storage requirements by a factor of two.(Figure 4)

This RF power data is stored in coincidence with all other data read out by the payload. This includes the fast waveform data as well as GPS determined orientation and temperature information. This allows additional cross-checks on the data from the high-speed waveform readout, immediately important for distinguishing and rejecting constant wave (CW) anthropogenic sources that would otherwise be convolved with the total broadband power.

Calibrated noise sources were injected into each signal channel immediately before each flight, allowing a normalization of differences due to process differences between the independent electronics in each channel. Additional pulsed noise sources were also injected to observe the ability of the electronics to react to a fast radiative object traversing the field of view of the detector.

6. Expected noise sources and limits

The primary source of background noise for the ANITA telescope is anthropomorphic sources, from both ground based transmitting stations and satellites in orbit above the detector. These sources are easily distinguishable from AQN annihilation interactions, by either CW rejection utilizing spectral information from fast-sampled digitized waveforms, or their enormously slower

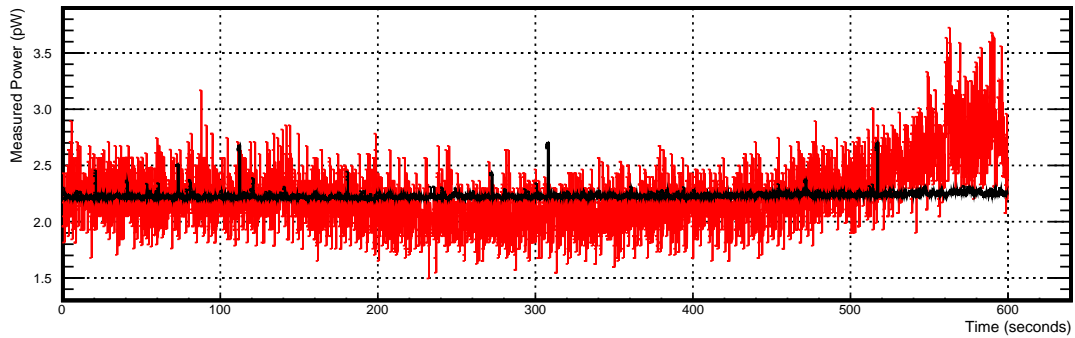


Figure 4: A comparison time series of measured power from the ANITA2 (red) and ANITA3 (black) flights. Easily visible is the decrease in noise from ANITA3’s improved power monitor subsystem

characteristic velocity. However, the increased radio flux density incident on the antennas from these noise sources limits their sensitivity to low mass or distant AQN events in the direction of the noise source while it is in the field of view.

An additional background signal is a similar magnitude moving thermal increase generated by meteors disintegrating in the atmosphere. The flux of that background is on a similar scale to the expected flux from AQN annihilation paths (see meteor measurements in Figure 1). However, the velocity distribution for meteors is a factor of 6 lower, yielding a possible discrimination cut. Meteors are typically observed in radio below 80km/s, while AQNs will be moving at the mean galactic velocity of 240km/s. These detectable meteoroids are comparable to the expected flux of AQN objects, and can be used as a calibration signal to determine the efficiency of any analysis.

7. Conclusion and Outlook

The ANITA balloon borne experiments provide a unique opportunity to probe a region of parameter space that may explain a fraction of the dark matter anomaly. Promising theoretical calculations provide a strong motivation for a further search of the previous flight data for AQN annihilation interactions occurring beyond the expected background rate from meteoric objects. With the return of the ANITA3 flight data in May of 2015, the search for this exotic physics particle can continue and set limits on its percentage of the dark matter fraction.

References

- [1] M. Bartlemann, Rev. Mod. Phys. 82, 331382 (2010).
- [2] P. Gorham, *Antiquark nuggets as dark matter: New constraints and detection prospects* arXiv:1208:3697
- [3] Wilczek et al., Phys. Lett. B 422, 247, 1998
- [4] E. Witten, Phys. Rev. D 30, 272 (1984).
- [5] D. T. Cumberbatch, G. D. Starkmann, J. Silk, PRD 77,063522.
- [6] A. H. G. Peter, M. Rocha, J. S. Bullock, M. Kaplinghat, arXiv:1208.3026, (2012).

- [7] M. M. Forbes, and A. R. Zhitnitsky, PRD 78, 083505, (2008).
- [8] M. M. Forbes, K. Lawson, and A. R. Zhitnitsky, PRD 82, 083510, (2010).
- [9] K. Lawson, PRD 83, 103520, (2011).
- [10] K. Lawson, arXiv:1208.0042 (2012).
- [11] G. Lugones, J. E. Horvath, Phys.Rev. D69 (2004) 063509.
- [12] P.W. Gorham et al. [The ANITA Collaboration], Astropart. Physics 32, 10-41, (2009).
- [13] P.W. Gorham, et al. *Observational Constraints on the Ultra-high Energy Cosmic Neutrino Flux from the Second Flight of the ANITA experiment* arXiv:1003.2961
- [14] P.W. Gorham, Private correspondence